SLAC-PUB-2564
July 1980
(A)

EVALUATION OF RADIATIVE SPIN POLARIZATION IN AN ELECTRON STORAGE RING*

Alexander W. Chao
Stanford Linear Accelerator Center
Stanford University, Stanford, California 94305

ABSTRACT

We have developed a matrix formalism that provides an accurate way of evaluating the degree of spin polarization built up through the process of synchrotron radiation under a wide variety of storage ring operation conditions.

I. Introduction

The value of an electron storage ring as a high energy physics research tool increased considerably since it was realized[1-7] that the spin polarization of a stored electron beam can potentially reach a level of 92% within a practical time scale. The mechanism for this polarization build-up is that, in a magnetic field, the spin transition rate from the up state to the down state is not equal to that from the down state to the up state during the process of synchrotron radiation. The beam accumulates a net polarization as a result.

(Submitted to Nuclear Instruments and Methods)

* Work supported by the Department of Energy under contract number DE-AC03-76SF00515

The existence of radiative spin polarization was soon confirmed experimentally in several existing electron storage rings.[4,8,9,10] The degree of polarization, however, was often found to be lower than the expected 92% due to depolarization effects. It turns out that the very mechanism that gives rise to polarization, namely the synchrotron radiation, is also the main cause for depolarization.[4-7,11] As an electron emits a photon during synchrotron radiation, it receives a recoil perturbation which excites its subsequent oscillatory orbital motions. The electron then sees a perturbing electromagnetic field, which is modulated by these orbital oscillations, causing its spin to precess accordingly. Summing over the uncorrelated photon-emission events results in a diffusion of spin direction which becomes serious when the spin motion couples strongly to the oscillatory orbital motion.

The achieved level of polarization is determined by an equilibrium between the polarizing and the depolarizing effects of synchrotron radiation. The strength of the polarizing effect is already well-known.[1-3] The depolarization strength, on the other hand, depends on details of the storage ring operation and is often difficult to calculate with accuracy. For a perfect storage ring with planar geometry, the spin-orbit coupling vanishes and the ideal 92% polarization is ensured. In the presence of imperfections or in storage rings designed with non-planar geometry, depolarization strength must be known accurately in order to estimate the achievable polarization. In this paper, we present a matrix formalism that fulfills this purpose for a wide variety of storage ring designs and operation conditions.

II. The Matrix Formalism

Here we briefly describe the basic idea of the matrix formalism. Detailed analyses are given in the following sections.

In order to calculate the depolarization strength, one needs to know how the spin and orbital degrees of freedom of an electron couple among themselves. It is well known that in order to fully describe the orbital motion of an electron, one needs six canonical coordinates (x, x', y, y', z, δ), where x, y and z are the horizontal, vertical and longitudinal displacements of a particle relative to the beam trajectory; $\delta = \Delta E/E_0$ is the relative energy error. In the linear approximation, the transformations of the six-dimensional vector are described by 6 x 6 transport matices.[12,13] Spin motion can be conveniently included by adding two more spin coordinates (α,β) to form 8-dimensional vectors, $X = (x_1, x_2, x_3, x_4, x_5, x_6, x_7, x_8) = (x, x', y, y', z, \delta, \alpha, \beta)$, and by generalizing the 6 x 6 transformations to 8 x 8.

The 8 x 8 matrix, T, which transforms X for one revolution of the storage ring, has four eigenstates: three orbital x, y, z-states and one spin state; each eigenstate being defined by a complex conjugate pair of eigenvectors of T. Any perturbation to the vector X, such as the recoil perturbation resulted from emitting a synchrotron photon, can be projected onto the four eigenstates. The projections onto the x, y, z-states give the contribution of this perturbation to the corresponding x, y, z-emittances, while the projection onto the spin state gives the contribution to spin diffusion. Since the same physical process of quantum emissions drives both the spin diffusion and the beam emittances of the electron beam, the matrix formalism offers the possibility of obtaining the spin diffusion rate and the 21 beam distribution parameters $<x_i x_j>$, $i,j=1,\ldots,6$, in one concise package.

One disadvantage of the matrix method is that nonlinear depolarization effects such as those caused by the perturbation of the beam-beam collisions or those associated with spreads in the orbital frequencies can not be included. Due to the intrinsic complexity involved, the nonlinear depolarization effects can only be evaluated very roughly by other methods.[14]

III. Describing Spin Motion By Matrices

We assume that the 6-dimensional closed-orbit vector $X_e = (x_e, x_e', y_e, y_e', z_e, \delta_e)$ in the presence of various perturbations has been obtained around the storage ring.[13]

An ideal electron will follow the closed-orbit exactly, experiencing well defined electric and magnetic fields, $\vec{E}(X_e)$ and $\vec{B}(X_e)$, in each of the beam-line elements. Spin precession caused by these EM fields can be described by 3 x 3 rotations. Explicit expressions for these 3 x 3 matrix transformations are given in Appendix I. Knowing the storage ring beam-line, one multiplies all 3 x 3 matrices successively to obtain the total spin precession transformation R_{tot} for one revolution around a certain position defined as s = 0. A right-handed orthonormal base $(\hat{n}, \hat{m}, \hat{\ell})$ with $\hat{n}$ rotation axis of R_{tot} is then chosen. Successive 3 x 3 transformations then bring this base to other positions with C > s > o, where C is the storage ring circumference. In one revolution, it gives

$$\begin{bmatrix} \hat{n} \\ \hat{m} \\ \hat{\ell} \end{bmatrix}_{s=C} = \begin{bmatrix} 1 & 0 & 0 \\ 0 & \cos 2\pi\nu & -\sin 2\pi\nu \\ 0 & \sin 2\pi\nu & \cos 2\pi\nu \end{bmatrix} \begin{bmatrix} \hat{n} \\ \hat{m} \\ \hat{\ell} \end{bmatrix}_{s=0} \qquad (1)$$

where $\exp(\pm i2\pi\nu)$ are the two nontrivial eigenvalues of R_{tot}. The quantity ν gives the spin precession wave number and $\hat{n}$ gives the direction of the net beam polarization. For a storage ring with planar geometry and without imperfections, ν is equal to $\gamma(g-2)/2$ with γ the Lorentz factor and g the gyromagnetic ratio of an electron and $\hat{n}$ coincides with the direction of the guiding magnetic field $\hat{y}$. In the presence of imperfections, $\hat{n}$ deviates from $\hat{y}$ noticeably if ν is close to an integer.

Once the base vectors are defined, the classical spin direction of a nearly polarized electron is written as:

$$\vec{S} \cong \hat{n} + \alpha\hat{m} + \beta\hat{\ell}, \quad |\alpha,\beta| << 1 \qquad (2)$$

The quantities α and β thus describe the spin to a linear approximation and $\frac{1}{2}(\alpha^2 + \beta^2)$ specifies the degree of depolarization of this electron.

The spin equation of motion of an electron is[15]

$$\frac{d}{ds} \vec{S} = \vec{\Omega}\,(X_e + X) \times \vec{S}, \qquad (3)$$

where the precession angular velocity $\vec{\Omega}$ depends on the position of the electron, $X_e + X$, with X_e the closed-orbit and X the oscillatory components relative to X_e. In a linear approximation, $\vec{\Omega}$ can be decomposed into $\vec{\Omega}(X_e) + \vec{\omega}(X)$, where $\vec{\Omega}(X_e)$ has already appeared in Appendix I and the perturbation ω is small compared with Ω. A list of $\vec{\omega}(X)$ for some beam-line elements is given in Table 1. We have assumed that the beam-line elements are short enough that X_e and X do not change appreciably within their lengths. We have also defined $\nu_o = \gamma(g-2)/2$.

Table 1: Explicit Expressions of $\vec{\omega}(X)$ for Various Beam-Line Elements.

Horizontal Bending Magnet, Horizontal Kicker	$\frac{B_y}{(B\rho)_o} [\delta\, \hat{y} + \nu_o y'\, \hat{z}]$
Vertical Bending Magnet, Vertical Kicker	$\frac{B_x}{(B\rho)_o} [\delta\, \hat{x} + \nu_o x'\, \hat{z}]$
Quadrupole	$-\frac{1+\nu_o}{(B\rho)_o} \frac{\partial B_y}{\partial x} [y\hat{x} + x\hat{y}]$
Skew Quadrupole	$-\frac{1+\nu_o}{(B\rho)_o} \frac{\partial B_y}{\partial y} [-x\, \hat{x} + y\, \hat{y}]$
RF Cavity	$-\frac{1+\nu_o}{(B\rho)_o} E_z [x'\, \hat{y} - y'\, \hat{x}]$
Sextupole	$-\frac{1+\nu_o}{(B\rho)_o} \frac{\partial^2 B_y}{\partial x^2} \left[(xy_e + yx_e)\hat{x} + (xx_e - yy_e)\hat{y}\right]$

Noting that $\hat{n}$, $\hat{m}$ and $\hat{\ell}$ satisfy

$$\frac{d}{ds} \vec{S} = \vec{\Omega}(X_e) \times \vec{S}, \tag{4}$$

one obtains by substituting Eq. (2) into Eq. (3) that

$$\begin{aligned} \frac{d}{ds} \alpha &\simeq \vec{\omega}\,(X) \cdot \hat{\ell} \\ \frac{d}{ds} \beta &\simeq -\vec{\omega}\,(X) \cdot \hat{m} \end{aligned} \tag{5}$$

If we now form an 8-dimensional state vector from the components of X:

$$\begin{bmatrix} x \\ x' \\ y \\ y' \\ z \\ \delta \\ \alpha \\ \beta \end{bmatrix} \tag{6}$$

the corresponding 8 x 8 transformation matrices would look like

$$\left[\begin{array}{c|c} \text{TRANSPORT} & 0 \\ \hline \text{D} & \begin{matrix} 1 & 0 \\ 0 & 1 \end{matrix} \end{array}\right] \tag{7}$$

where TRANSPORT means the usual 6 x 6 transport matrices describing the transformation among the orbital coordinates; the upper right corner is a 6 x 2 matrix filled by 0's; the 2 x 6 matrix D is obtained from Table 1 and Eq. (5). Explicit expressions of the 8 x 8 matrices, including the D matrices, for some beam-line elements are given in Appendix II.

One must not forget that, due to the discontinuous transition in the definition of the base vectors as the electron travels across $s = C$ [See Eq. (1)], an extra transformation for the spin components is required at an infinitesimal distance before $s = C$:

$$\begin{bmatrix} \alpha \\ \beta \end{bmatrix}_{s=C} = \begin{bmatrix} \cos 2\pi\nu & \sin 2\pi\nu \\ -\sin 2\pi\nu & \cos 2\pi\nu \end{bmatrix} \begin{bmatrix} \alpha \\ \beta \end{bmatrix}_{s=C^-} \tag{8}$$

Starting from any position s we multiply all transformation matrices successively around the beam-line to obtain a transformation matrix for one revolution. It will be designated as $T(s)$. Let the eigenvalues and eigenvectors of $T(s)$ be λ_k and $E_k(s)$, respectively, with

$$\begin{aligned} T(s)\, E_k\,(s) &= \lambda_k\, E_k\,(s) \\ \lambda_k^{\;*} &= \lambda_{-k} \\ E_k^{\;*} &= E_{-k}\,, \quad k = \pm\mathrm{I},\ \pm\mathrm{II},\ \pm\mathrm{III},\ \pm\mathrm{IV}. \end{aligned} \tag{9}$$

Eigenvectors at other positions, $E_k(s')$, are obtained from $E_k(s)$ by successive transformations from s to s'. The spin eigenstates E_{IV} and E_{-IV} contain only spin components and no orbital components. The IV-th eigenvalue is given by $\lambda_{IV} = \exp(i2\pi\nu)$ with ν the spin tune.

It is not necessary to normalize the spin eigenstates since they are not used in later calculations. The orbital eigenstates are normalized by

$$\tilde{e}_{\pm k}^{\;*}\, S e_{\pm k} = \pm i, \quad k = \mathrm{I},\ \mathrm{II},\ \mathrm{III}, \tag{10}$$

where e_k' is the 6-dimensional vector whose components are the six orbital components of E_k and

$$S = \begin{bmatrix} 0 & -1 & 0 & 0 & 0 & 0 \\ 1 & 0 & 0 & 0 & 0 & 0 \\ 0 & 0 & 0 & -1 & 0 & 0 \\ 0 & 0 & 1 & 0 & 0 & 0 \\ 0 & 0 & 0 & 0 & 0 & -1 \\ 0 & 0 & 0 & 0 & 1 & 0 \end{bmatrix} \qquad (11)$$

IV. Evaluation of Polarization

The spin polarization in an electron storage ring approaches the equilibrium value P_o with a polarization time constant τ_p. The polarization of an initially unpolarized beam is equal to $P_o[1 - \exp(-t/\tau_p)]$. It has been shown that P_o and τ_p are given by[11]

$$P_o = \frac{8}{5\sqrt{3}} \frac{\alpha_-}{\alpha_+}$$

$$\tau_p^{-1} = \frac{5\sqrt{3}}{8} \frac{r_e \hbar \gamma^5}{m_e} \alpha_+ \qquad (12)$$

where r_e is the classical radius of an electron, $\hbar$ is Planck's constant divided by 2π, m_e is the rest mass of an electron and

$$\alpha_+ = \frac{1}{C} \oint \frac{ds}{|\rho(s)|^3} \left[1 - \frac{2}{9} (\hat{n} \cdot \hat{v})^2 + \frac{11}{18} \left| \gamma \frac{\partial \hat{n}}{\partial \gamma} \right|^2 \right]_s$$

$$\alpha_- = \frac{1}{C} \oint \frac{ds}{|\rho(s)|^3} \left[\frac{\dot{\hat{v}} \times \hat{v}}{|\dot{\hat{v}}|} \cdot (\hat{n} - \gamma \frac{\partial \hat{n}}{\partial \gamma}) \right]_s \qquad (13)$$

In Eq. (13), C is the storage ring circumference, $\rho(s)$ is the bending radius of the magnetic field seen by the particle, $\hat{v}$ is the instantaneous velocity unit vector, $\hat{n}$ is the polarization direction described before. The crucial quantity $\gamma\, \partial\hat{n}/\partial\gamma$ in Eq. (13) is, in the matrix language, the projection of the recoil perturbation when emitting a synchrotron photon onto the spin eigenstate. A proper calculation of $\gamma\, \partial\hat{n}/\partial\gamma$ takes into account the spin-orbit coupling as a result of a sudden loss in particle energy due to emitting a synchrotron photon. In particular, the strongest spin-orbit coupling occurs when the spin wave number ν is close to $k \pm \nu_{x,y,s}$ for some integer k, where $\nu_{x,y,s}$ are the wave numbers[16] for the horizontal-betatron, the vertical-betatron, and the synchrotron orbital motions, respectively. These depolarization resonances are included only if the correct definition of $\gamma\, \partial\hat{n}/\partial\gamma$ is used.

Consider a fully polarized ideal electron. Let a photon be emitted at s with energy deviating from the mean value by a random amount δE. After emission, the electron is left in the state

$$X(s) = \begin{bmatrix} 0 \\ 0 \\ 0 \\ 0 \\ 0 \\ 0 \\ -\delta E/E_o \\ 0 \\ 0 \end{bmatrix} \tag{14}$$

Decomposing into eigenstates, one has

$$\begin{aligned} X(s) &= \sum_k A_k E_k(s) \\ &= \sum_{k=\pm I,\ \pm II,\ \pm III} A_k E_k(s) + \begin{bmatrix} 0 \\ 0 \\ 0 \\ 0 \\ 0 \\ 0 \\ \alpha \\ \beta \end{bmatrix}_s \end{aligned} \tag{15}$$

where we have used the property that the spin eigenstates $E_{\pm IV}$ contain no orbital coordinates. The value for A_k for $k = \pm I, \pm II, \pm III$ can be obtained by equating the orbital components on both sides of Eq. (15). It has been found [13] that

$$A_k = -i \frac{\delta E}{E_o} E_{5k}^* (s), \quad k = I, II, III \tag{16}$$

with $A_{-k} = A_k^*$ and E_{jk} the j-th component of vector E_k.

Equating the spin components of Eq. (15) then yields

$$\begin{bmatrix} \overline{\alpha} \\ \\ \overline{\beta} \end{bmatrix}_s = -2 \frac{\delta E}{E_o} \sum_k{}' \begin{bmatrix} \mathrm{Im}\ (E_{5k}^* E_{7k}) \\ \\ \mathrm{Im}\ (E_{5k}^* E_{8k}) \end{bmatrix}_s \tag{17}$$

where $\sum_k{}'$ means summation with k running over I, II and III only. After the photon emission event, the orbital eigenstates are rapidly damped by the radiation damping[17], while the spin components precess with initial values given by Eq. (17). The quantity $\gamma \frac{\partial \hat{n}}{\partial \gamma}$ at position s is then simply

$$\left(\gamma \frac{\partial \hat{n}}{\partial \gamma}\right)_s = -2 \sum_k{}' \left[\mathrm{Im}(E_{5k}^* E_{7k})\hat{m} + \mathrm{Im}(E_{5k}^* E_{8k})\hat{\ell}\right]_s . \tag{18}$$

Knowing the eigenvectors $E_k(s)$ of the 8 x 8 transformation matrices around the storage ring thus allows a calculation of P_o and τ_p according to Eq. (12).

IV. Estimate for the SPEAR Storage Ring

A computer code has been prepared for the polarization and beam distribution calculations for SPEAR. The thin-lens approximation has been used. The beam-line elements for the ideal SPEAR lattice include horizontal bending magnets, quadrupole magnets, sextupole magnets, rf cavities and drift spaces. Without field imperfections, the ideal lattice produces an equilibrium polarization of 92%. To simulate field imperfections, we introduce a random distribution of vertical orbit kickers. The resulting vertical closed orbit distortion makes sextupoles behave like skew quadrupoles and quadrupoles behave like additional vertical kickers. In the presence of these field imperfections, the degree of polarization P_o is plotted in Fig. 1 as a function of the beam energy E_o.

The SPEAR lattice used in Fig. 1 is specified by the lattice parameters: $\nu_x = 5.28$, $\nu_y = 5.18$, $\nu_s = .022$, $\beta_x^* = 1.2$ m, $\beta_y^* = .10$m and $\eta_x^* = 0$, where β_x^*, β_y^* and η_x^* are[16] the usual horizontal beta-function, vertical beta-function and the energy dispersion function at the interaction points. The strengths of the vertical kickers are normalized such that the rms closed orbit distortion after orbit correction is Δy_{rms} = 1.2mm, which is typical for SPEAR operation.

Locations of the depolarization resonances are indicated by arrows at the top of Fig. 1. Each integer resonance, ν = integer, is surrounded by six sideband resonances, $\nu \pm \nu_{x,y,s}$ = integer. The integer resonances and the two associated synchrotron sideband resonances overlap and are shown as single depolarization dips in Fig. 1. The width of the region covered by an integer resonance alone is typically less than 10^{-3} in ν units. For different distributions of vertical kickers whose strengths are normalized so that the orbit distortion after correction has Δy_{rms} = 1.2mm, the qualitative behavior of P_o vs E_o does not change much from that shown in Fig. 1.

Acknowledgements

The author is obliged to Professors Roy Schwitters and Ya S. Derbenev for many stimulating discussions.

References

1) I. M. Ternov, Yu. M. Lokutov and L. I. Korovina, Sov. Phys. JETP 14, 921 (1962).

2) A. A. Sokolov and I. M. Ternov, Sov. Phys. Dokl. 8, 1203 (1964).

3) J. D. Jackson, Rev. Mod. Phys. 48, 417 (1976).

4) V. N. Baier, Sov. Phys. Uspekhi 14, 695 (1972).

5) Ya. S. Derbenev and A. M. Kondratenko, Sov. Phys. JETP 35, 230 (1972).

6) R. F. Schwitters, Nucl. Instru. and Meth. 117, 331 (1974).

7) Ya. S. Derbenev, A. M. Kondratenko and A. N. Skrinsky, Part. Accel. 9, 247 (1979).

8) D. Potaux, Proc. 8-th Intern. Conf. on High Energy Accel., CERN, 1971, p. 127.

9) U. Camerini et. al., Phys. Rev. D12, 1855 (1975).

10) D. B. Gustavson, et. al., Nucl. Instru. and Meth. 165, 177 (1979).

11) Ya. S. Derbenev and A. M. Konratenko, Sov. Phys. JETP 37, 968 (1973).

12) Karl Brown, SLAC Report 75 (1967).

13) A. W. Chao, J. Appl. Phys. 50, 595 (1979).

14) A. M. Kondratenko, Sov. Phys. JETP 39, 592 (1974).

15) V. Bargman, L. Michel and V. L. Telegdi, Phys. Rev. Lett. 2, 435 (1959).

16) E. D. Courant and H. S. Snyder, Ann. Phys. 3, 1 (1958).

17) M. Sands, SLAC Report 121 (1970).

APPENDIX I. SPIN PRECESSION IN UNIFORM EM FIELDS

The equation for spin precession is

$$\frac{d}{ds}\vec{S} = \vec{\Omega} \times \vec{S} \qquad \text{(I.1)}$$

where $\vec{\Omega}$ is related to EM fields by[15]

$$\vec{\Omega} = -\frac{1}{(B\rho)_o}\Big[(\nu_o + 1 - \delta)(\vec{B} - \hat{v} \times \vec{E}) - \nu_o\, \hat{v}(\hat{v} \cdot \vec{B})\Big] \qquad \text{(I.2)}$$

with $\nu_o = \gamma(g-2)/2$ and $\delta = \Delta E/E_o$.

For an ideal electron with trajectory $X_e = (x_e, x_e', y_e, y_e', z_e, \delta_e)$, $\vec{\Omega}(X_e)$ for various beam-line elements are listed in Table 2. Assuming X_e does not change appreciably within the length of a beam-line element, we regard $\vec{\Omega}(X_e)$ as being uniform.

The transformation matrix which transforms the spin components as the particle travels through a distance s in a uniform EM field is given by

$$\begin{bmatrix} S_x \\ S_y \\ S_z \end{bmatrix}_f = \begin{bmatrix} \alpha^2(1-C)+C & \alpha\beta(1-C)-\gamma S & \alpha\gamma(1-C)+\beta S \\ \alpha\beta(1-C)+\gamma S & \beta^2(1-C)+C & \beta\gamma(1-C)-\alpha S \\ \alpha\gamma(1-C)-\beta S & \beta\gamma(1-C)+\alpha S & \gamma^2(1-C)+C \end{bmatrix} \begin{bmatrix} S_x \\ S_y \\ S_z \end{bmatrix}_i \qquad \text{(I.3)}$$

where α, β and γ are the direction cosines $\hat{\Omega}\cdot\hat{x}$, $\hat{\Omega}\cdot\hat{y}$ and $\hat{\Omega}\cdot\hat{z}$; and

$$C = \cos(\Omega s) \qquad S = \sin(\Omega s).$$

Using Table 2 for $\vec{\Omega}$, one thus obtains the 3 x 3 matrice which transforms the spin components of an ideal electron through a given EM element.

APPENDIX II. GENERALIZED TRANSPORT MATRICES

The generalized transport matrices for the state vector (x, x', y, y', z, δ, α, β) are listed below for various beam-line elements. Thin-lens approximation has been used. For the rf cavity, ϕ_s is the synchronous phase[16] and $\hat{V}$ is the peak voltage.

Drift Space

$$\begin{bmatrix} 1 & \ell & 0 & 0 & 0 & 0 & 0 & 0 \\ 0 & 1 & 0 & 0 & 0 & 0 & 0 & 0 \\ 0 & 0 & 1 & \ell & 0 & 0 & 0 & 0 \\ 0 & 0 & 0 & 1 & 0 & 0 & 0 & 0 \\ 0 & 0 & 0 & 0 & 1 & 0 & 0 & 0 \\ 0 & 0 & 0 & 0 & 0 & 1 & 0 & 0 \\ 0 & 0 & 0 & 0 & 0 & 0 & 1 & 0 \\ 0 & 0 & 0 & 0 & 0 & 0 & 0 & 1 \end{bmatrix} \tag{II.1}$$

Horizontal Bend Magnet or Kicker : $q = B_y \ell/(B\rho)_o$

$$\begin{bmatrix} 1 & 0 & 0 & 0 & 0 & 0 & 0 & 0 \\ 0 & 1 & 0 & 0 & 0 & q & 0 & 0 \\ 0 & 0 & 1 & 0 & 0 & 0 & 0 & 0 \\ 0 & 0 & 0 & 1 & 0 & 0 & 0 & 0 \\ -q & 0 & 0 & 0 & 1 & 0 & 0 & 0 \\ 0 & 0 & 0 & 0 & 0 & 1 & 0 & 0 \\ 0 & 0 & 0 & \nu_o q \ell_z & 0 & q\ell_y & 1 & 0 \\ 0 & 0 & 0 & -\nu_o q m_z & 0 & -qm_y & 0 & 1 \end{bmatrix} \tag{II.2}$$

Vertical Bend Magnet or Kicker : $q = B_x \ell/(B\rho)_o$

$$\begin{bmatrix} 1 & 0 & 0 & 0 & 0 & 0 & 0 & 0 \\ 0 & 1 & 0 & 0 & 0 & 0 & 0 & 0 \\ 0 & 0 & 1 & 0 & 0 & 0 & 0 & 0 \\ 0 & 0 & 0 & 1 & 0 & -q & 0 & 0 \\ 0 & 0 & q & 0 & 1 & 0 & 0 & 0 \\ 0 & 0 & 0 & 0 & 0 & 1 & 0 & 0 \\ 0 & q\nu_o \ell_z & 0 & 0 & 0 & q\ell_x & 1 & 0 \\ 0 & -q\nu_o m_z & 0 & 0 & 0 & -qm_x & 0 & 1 \end{bmatrix} \tag{II.3}$$

Quadrupole : $q = \frac{\ell}{(B\rho)_o} \frac{\partial}{\partial x} B_y$

$$\begin{bmatrix} 1 & 0 & 0 & 0 & 0 & 0 & 0 & 0 \\ -q & 1 & 0 & 0 & 0 & qx_e & 0 & 0 \\ 0 & 0 & 1 & 0 & 0 & 0 & 0 & 0 \\ 0 & 0 & q & 1 & 0 & -qy_e & 0 & 0 \\ -qx_e & 0 & qy_e & 0 & 1 & 0 & 0 & 0 \\ 0 & 0 & 0 & 0 & 0 & 1 & 0 & 0 \\ -(1+\nu_o)q\ell_y & 0 & -(1+\nu_o)q\ell_x & 0 & 0 & 0 & 1 & 0 \\ (1+\nu_o)qm_y & 0 & (1+\nu_o)qm_x & 0 & 0 & 0 & 0 & 1 \end{bmatrix} \qquad (II.4)$$

Skew Quadrupole : $q = \frac{\ell}{(B\rho)_o} \frac{\partial}{\partial y} B_y$

$$\begin{bmatrix} 1 & 0 & 0 & 0 & 0 & 0 & 0 & 0 \\ 0 & 1 & -q & 0 & 0 & qy_e & 0 & 0 \\ 0 & 0 & 1 & 0 & 0 & 0 & 0 & 0 \\ -q & 0 & 0 & 1 & 0 & qx_e & 0 & 0 \\ -qy_e & 0 & -qx_e & 0 & 1 & 0 & 0 & 0 \\ 0 & 0 & 0 & 0 & 0 & 1 & 0 & 0 \\ (1+\nu_o)q\ell_x & 0 & -(1+\nu_o)q\ell_y & 0 & 0 & 0 & 1 & 0 \\ -(1+\nu_o)qm_x & 0 & (1+\nu_o)qm_y & 0 & 0 & 0 & 0 & 1 \end{bmatrix} \qquad (II.5)$$

RF Cavity : $q = 2\pi\ e\ \hat{V} \cos\phi_s / C\ E_o\ ;\ r = (1+\nu_o)\ e\ \hat{V} \sin\phi_s / E_o$

$$\begin{bmatrix} 1 & 0 & 0 & 0 & 0 & 0 & 0 & 0 \\ 0 & 1 & 0 & 0 & 0 & 0 & 0 & 0 \\ 0 & 0 & 1 & 0 & 0 & 0 & 0 & 0 \\ 0 & 0 & 0 & 1 & 0 & 0 & 0 & 0 \\ 0 & 0 & 0 & 0 & 1 & 0 & 0 & 0 \\ 0 & 0 & 0 & 0 & q & 1 & 0 & 0 \\ 0 & -r\ell_y & 0 & r\ell_x & 0 & 0 & 1 & 0 \\ 0 & rm_y & 0 & -rm_x & 0 & 0 & 0 & 1 \end{bmatrix} \qquad (II.6)$$

Sextupole : $q = \frac{\ell}{(B\rho)_o} \frac{\partial^2}{\partial x^2} B_y$; $r = (1+\nu_o)q$

$$\begin{bmatrix} 1 & 0 & 0 & 0 & 0 & 0 & 0 & 0 \\ -qx_e & 1 & qy_e & 0 & 0 & \frac{q}{2}(x_e^2-y_e^2) & 0 & 0 \\ 0 & 0 & 1 & 0 & 0 & 0 & 0 & 0 \\ qy_e & 0 & qx_e & 1 & 0 & -qx_e y_e & 0 & 0 \\ -\frac{q}{2}(x_e^2-y_e^2) & 0 & qx_e y_e & 0 & 1 & 0 & 0 & 0 \\ 0 & 0 & 0 & 0 & 0 & 1 & 0 & 0 \\ -r(y_e \ell_x + x_e \ell_y) & 0 & -r(x_e \ell_x - y_e \ell_y) & 0 & 0 & 0 & 1 & 0 \\ r(y_e m_x + x_e m_y) & 0 & r(x_e m_x - y_e m_y) & 0 & 0 & 0 & 0 & 1 \end{bmatrix} \quad \text{(II.7)}$$

Table 2: Explicit Expression of $\vec{\Omega}\,(X_e)$ for Various Beam-Line Elements

Horizontal Bending Magnet	$-\frac{B_y}{(B\rho)_o}\left[(\nu_o - \delta_e)\,\hat{y} - \nu_o y_e'\,\hat{z}\right]$
Vertical Bending Magnet	$-\frac{B_x}{(B\rho)_o}\left[(\nu_o - \delta_e)\,\hat{x} - \nu_o x_e'\,\hat{z}\right]$
Quadrupole	$-\frac{1+\nu_o}{(B\rho)_o}\,\frac{\partial B_y}{\partial x}\left[y_e\,\hat{x} + x_e\hat{y}\right]$
Skew Quadrupole	$-\frac{1+\nu_o}{(B\rho)_o}\,\frac{\partial B_y}{\partial y}\left[-x_e\hat{x} + y_e\hat{y}\right]$
RF Cavity	$-\frac{1+\nu_o}{(B\rho)_o}\,E_z\left[x_e'\hat{y} - y_e'\hat{x}\right]$
Horizontal Kicker	$-\frac{B_y}{(B\rho)_o}\left[(\nu_o + 1 - \delta_e)\,\hat{y} - \nu_o y_e'\,\hat{z}\right]$
Vertical Kicker	$-\frac{B_x}{(B\rho)_o}\left[(\nu_o + 1 - \delta_e)\hat{x} - \nu_o x_e'\,\hat{z}\right]$
Sextupole	$-\frac{1+\nu_o}{(B\rho)_o}\,\frac{\partial^2 B_y}{\partial x^2}\left[x_e y_e\,\hat{x} + \frac{1}{2}(x_e^2 - y_e^2)\hat{y}\right]$

Figure Caption

Fig. 1. Polarization P_o versus beam energy E_o for a typical SPEAR Configuration.

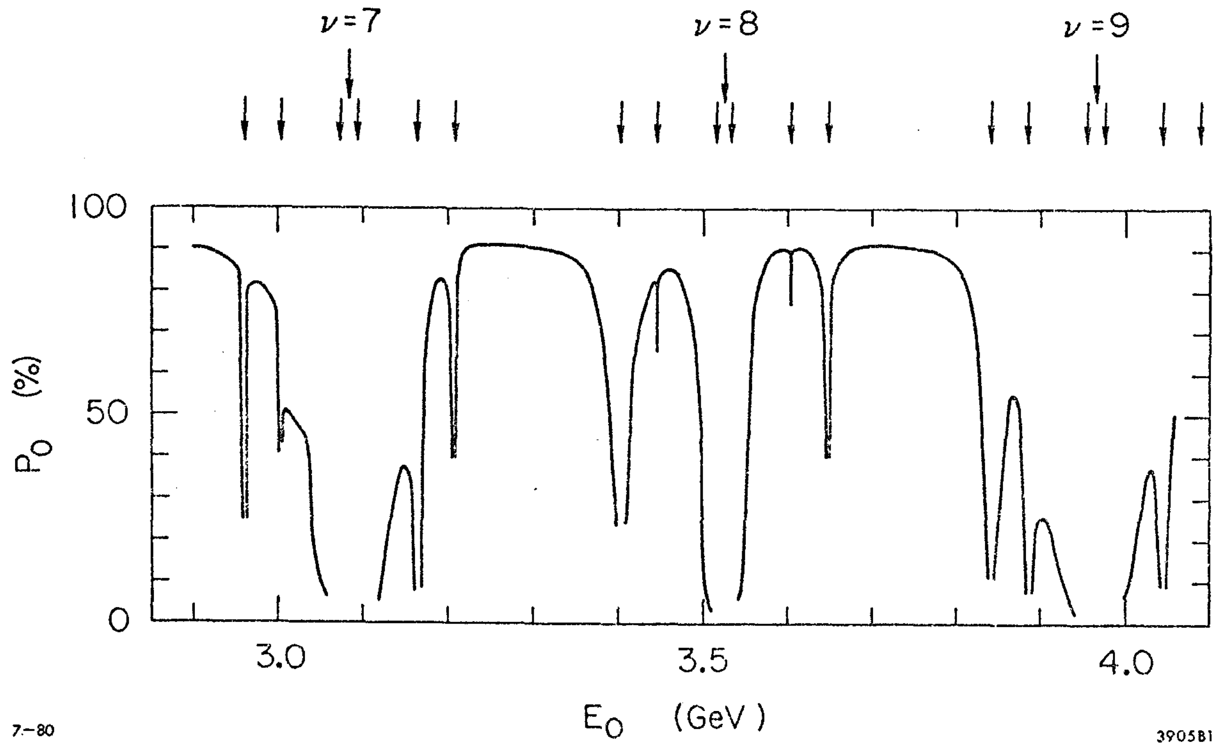

Fig. 1